

# DREAMVAR: TAMING REINFORCED VISUAL AUTOREGRESSIVE MODEL FOR HIGH-FIDELITY SUBJECT-DRIVEN IMAGE GENERATION

Xin Jiang<sup>1\*</sup> Jingwen Chen<sup>3</sup> Yehao Li<sup>3</sup> Yingwei Pan<sup>3</sup> Kezhou Chen<sup>2</sup> Zechao Li<sup>1†</sup> Ting Yao<sup>3</sup> Tao Mei<sup>3</sup>

<sup>1</sup> Nanjing University of Science and Technology <sup>2</sup> University of Science and Technology of China  
<sup>3</sup> HiDream.ai Inc.

## ABSTRACT

Recent advances in subject-driven image generation using diffusion models have attracted considerable attention for their remarkable capabilities in producing high-quality images. Nevertheless, the potential of Visual Autoregressive (VAR) models, despite their unified architecture and efficient inference, remains underexplored. In this work, we present DreamVAR, a novel framework for subject-driven image synthesis built upon a VAR model that employs next-scale prediction. Technically, multi-scale features of the reference subject are first extracted by a visual tokenizer. Instead of interleaving these conditional features with target image tokens across scales, our DreamVAR pre-fills the full subject feature sequence prior to predicting target image tokens. This design simplifies autoregressive dependencies and mitigates the train-test discrepancy in multi-scale conditioning scenario within the VAR paradigm. DreamVAR further incorporates reinforcement learning to jointly enhance semantic alignment and subject consistency. Extensive experiments demonstrate that DreamVAR achieves superior appearance preservation compared to leading diffusion-based methods.

**Index Terms**— Subject-Driven Image Generation, Visual Autoregressive Model

## 1. INTRODUCTION

Subject-driven image generation constitutes a fundamental task in visual generation, requiring models to follow textual prompts while faithfully preserving the visual appearance of reference subjects. While numerous efforts [1, 2, 3, 4, 5, 6, 7] have been dedicated to achieving high-quality subject customization using diffusion models, the potential of Visual Autoregressive (VAR) models for such fine-grained controllability remains largely underexplored. Accordingly, this work focuses on VAR models for subject-driven synthesis.

Generally, VAR models [8, 9, 10] define autoregressive learning in image generation as next-scale prediction or next-resolution prediction. Compared to raster-scan autoregressive (AR) models [11], masked AR models [12, 13] and diffusion

models [14, 15, 16], VAR models achieve faster inference speed. Moreover, the unified architecture of VAR models enables flexible integration of additional modalities. Recent efforts have aimed at improving the controllability of VAR models. ControlVAR [17] extends a VAR model to condition image generation on structural signals such as edges or depth maps. Furthermore, ARbooth [18] tackles customized image generation by fine-tuning selective layers and subject-specific text embeddings within a VAR model. Although effective, this approach necessitates per-subject optimization, incurring significant computational overhead for practical deployment.

To overcome the above limitations and leverage the merits of VAR models, we present a novel framework named DreamVAR, as shown in Fig. 1 (a). Within the next-scale prediction paradigm, a straightforward way [17] to inject reference conditions is to concatenate them with the target image tokens at their corresponding scales. However, we found that this trivial strategy led to suboptimal results. We argue that this is due to the train-test discrepancy: model predictions are conditioned on ground-truth history during training, but on generated image tokens in inference. This impact would be further amplified by interleaving unchanged conditional tokens with target image tokens across scales. To mitigate this discrepancy, our DreamVAR pre-fills the multi-scale features of the reference subject extracted by a visual tokenizer before initiating autoregressive generation. Inspired by the success of leveraging reinforcement learning in LLMs [19, 20], we incorporate Group Relative Policy Optimization (GRPO) [19] into our DreamVAR with multiple rewards for subject consistency and semantic alignment (shown in Fig. 1 (b)), which finally improves generation quality. Extensive experiments show that our DreamVAR achieves strong subject consistency, surpassing leading diffusion-based models.

## 2. METHODOLOGY

### 2.1. Preliminary: Next-Scale Prediction

Visual Autoregressive (VAR) models [8, 9] reformulate the autoregressive process from next-token prediction to next-scale prediction. Formally, let  $\mathbf{I} = (\mathbf{I}_1, \mathbf{I}_2, \dots, \mathbf{I}_K)$  denote token maps of  $K$  different resolutions or scales for an image,

\*This work was performed at Hidream.ai Inc.

†Corresponding Author: zechao.li@njust.edu.cn

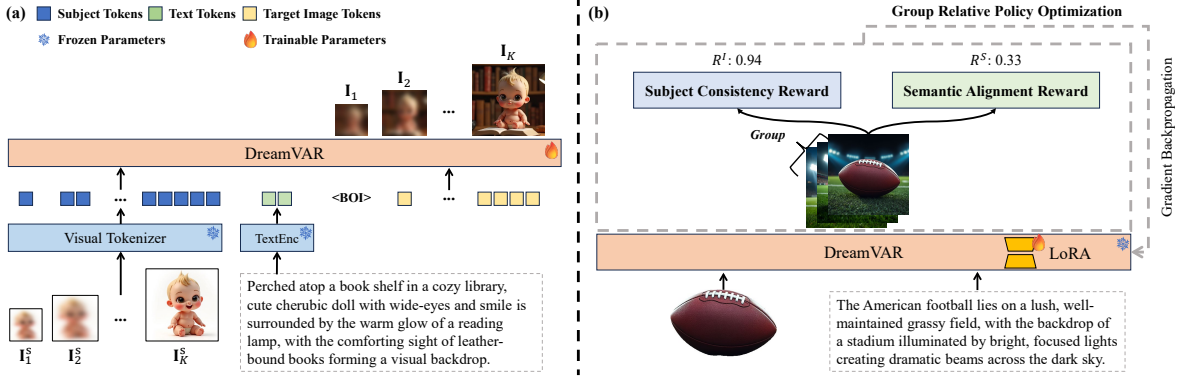


**Fig. 1.** (a) The framework of our DreamVAR for subject-driven image generation, which alleviates the train-test discrepancy through subject feature pre-filling. (b) The pipeline of reinforcement learning with GRPO in our DreamVAR.

the autoregressive likelihood of VAR models is defined as:

$$p(\mathbf{I}_1, \mathbf{I}_2, \dots, \mathbf{I}_K) = \prod_{k=1}^K p(\mathbf{I}_k | \mathbf{I}_{<k}, \mathbf{C}), \quad (1)$$

where  $\mathbf{C}$  denotes extra conditions for image generation (e.g., text prompt). Practically, the 2D spatial token map  $\mathbf{I}_k$  is usually flattened into a 1D token sequence for computation.

## 2.2. DreamVAR

Our proposed DreamVAR for subject-driven image generation builds upon a pre-trained text-to-image VAR model (Infinity [8]), which employs multi-scale visual tokenizer and bitwise self-correction to improve generation quality. Please refer to [8] for more details about Infinity.

As described previously in the introduction, VAR models tend to suffer from the train-test discrepancy due to teacher-forcing training schema. This impact would be amplified in multi-scale conditional generation when trivially interleaving conditional tokens with target image tokens, leading to degraded performance. To overcome this, we propose pre-filling all the conditional tokens of the reference subject prior to the autoregressive prediction of target image tokens. The overall framework is illustrated in Fig.1 (a).

Specifically, our DreamVAR extracts multi-scale features  $\mathbf{I}^s = (\mathbf{I}_1^s, \mathbf{I}_2^s, \dots, \mathbf{I}_K^s)$  of the reference subject using the visual tokenizer of the pre-trained VAR model, which capture fine-grained details of the reference subject. Then,  $\mathbf{I}^s$  is left-padded to the text tokens  $\mathbf{C}^t$  and all target image token maps  $\mathbf{I}$ , leading to  $(\mathbf{I}_1^s, \mathbf{I}_2^s, \dots, \mathbf{I}_K^s, \mathbf{C}^t, \mathbf{I}_1, \mathbf{I}_2, \dots, \mathbf{I}_K)$ . Compared to the interleaved conditioning strategy  $(\mathbf{C}^t, \mathbf{I}_1^s, \mathbf{I}_1, \mathbf{I}_2^s, \mathbf{I}_2, \dots, \mathbf{I}_K^s, \mathbf{I}_K)$  used in [17], our design simplifies autoregressive dependencies and eliminates the need for joint control-image modeling. Finally, we enforce full conditioning on  $(\mathbf{I}^s, \mathbf{C}^t)$  and causal dependence on previous scales  $(\mathbf{I}_1, \mathbf{I}_2, \dots, \mathbf{I}_{k-1})$  for the prediction of  $\mathbf{I}_k$  through attention masking. This allows VAR model to effectively leverage multi-scale control signals from the reference subject at each scale while preserving its native next-scale prediction paradigm.

## 2.3. Multi-Reward Reinforcement Learning

Since both subject consistency and semantic alignment are critical for subject-driven image generation, we further incorporate Group Relative Policy Optimization (GRPO) [19] to fine-tune our DreamVAR, which significantly enhances the generation quality. The process is shown in Fig. 1 (b). Specifically, for a given text prompt  $c^t$  and a reference subject  $c^s$ , a group of  $G$  images  $\{o_i\}_{i=1}^G$  is sampled from the old policy  $\pi_{\theta_{old}}$  (i.e., the old version of our DreamVAR). Each generated image  $o_i$  is evaluated by reward functions to obtain the corresponding reward  $R_i$ . The advantage of  $o_i$  is then calculated by normalizing its reward using statistics of the group rewards  $\{R_i\}_{i=1}^G$ :

$$A_i = \frac{R_i - \text{mean}(\{R_i\}_{i=1}^G)}{\text{std}(\{R_i\}_{i=1}^G)}. \quad (2)$$

The training objective of GRPO can be formalized as:

$$\begin{aligned} \mathcal{J}_{\text{GRPO}}(\theta) = & \mathbb{E}_{c \sim C, \{o_i\}_{i=1}^G \sim \pi_{\theta_{old}}(\cdot | c)} \left[ \frac{1}{\sum_{i=1}^G |o_i|} \sum_{i=1}^G |o_i| \right. \\ & \left( \min(r_{i,t}(\theta)A_i, \text{clip}(r_{i,t}(\theta), 1 - \epsilon, 1 + \epsilon)A_i) \right. \\ & \left. \left. - \beta D_{\text{KL}}(\pi_{\theta} \| \pi_{\text{ref}}) \right) \right], \end{aligned} \quad (3)$$

where  $r_{i,t}(\theta) = \frac{p_{\theta}(o_{i,t}|c)}{p_{\theta_{old}}(o_{i,t}|c)}$ ,  $c = (c^t, c^s)$ .  $D_{\text{KL}}(\pi_{\theta} \| \pi_{\text{ref}})$  measures KL-divergence between the current policy  $\pi_{\theta}$  and the reference model  $\pi_{\text{ref}}$  (i.e., the frozen version of our DreamVAR), and  $\beta$  is the weighting coefficient.  $|o_i|$  denotes the length of the generated image token sequence.

Two rewards are devised to jointly enhance appearance preservation and image-text alignment during GRPO training: **Semantic Alignment Reward ( $R^S$ )**: This reward measures image-text alignment by computing the cosine similarity between the generated image and text prompt using CLIP.

**Subject Consistency Reward ( $R^I$ )**: This reward evaluates the preservation of visual details by computing cosine similarity between the subject of the generated image and reference subject in visual feature space such as [21, 22]. Particularly,

the generated and reference subjects are segmented before the reward calculation to minimize the impact of the background.

The final reward  $R$  for each generated image is a weighted combination of  $R^I$  and  $R^S$ , defined as:

$$R = \alpha R^I + \gamma R^S, \quad (4)$$

where  $\alpha$  and  $\gamma$  are trade-off coefficients.

## 2.4. Multi-Stage Training

We adopt a multi-stage training strategy to progressively optimize our DreamVAR as follows:

**Stage 1: Task Adaptation.** In the first stage, we extend the text-to-image VAR model to support subject-driven image generation by employing full fine-tuning on Subject-200K.

**Stage 2: Supervised Fine-Tuning.** After task adaptation, we observe that the visual quality of generated images is unsatisfactory, primarily due to low image fidelity in Subject-200K. Therefore, we curate a high-quality dataset (**DreamSubject-14K**) for supervised fine-tuning of DreamVAR.

**Stage 3: Reinforcement Learning.** In the final stage, GRPO is applied to further optimize our DreamVAR initialized from the previous stage using subject consistency reward and semantic alignment reward.

## 3. EXPERIMENTS

### 3.1. Experiments Setup

**Datasets.** Our DreamVAR is trained on Subject-200K [3] to establish the initial capability of subject-driven generation. To obtain DreamSubject-14K for supervised fine-tuning and reinforcement learning, we first use [23] to generate diverse descriptions for each category from Object365 [24]. For each description, a text-to-image model [25] is utilized to generate 5 images. Low-quality images are filtered using [26]. The remaining images and the categories of the corresponding objects in the images are fed into an open-vocabulary detector [27] for subject localization, which are further refined by [28] to produce precisely segmented subjects. Images that fail either object detection or segmentation are discarded.

**Implementation Details.** We build our DreamVAR upon Infinity-2B [8] by adapting it for subject-driven image generation via multi-stage training described in Sec.2.4 at a resolution of  $512 \times 512$ . In the first stage of task adaptation, the model is trained for 5,000 steps with a batch size of 16 per GPU and a learning rate of  $1 \times 10^{-5}$ . The model is fine-tuned for another 1,000 steps with a learning rate of  $1 \times 10^{-4}$  in the second stage (i.e., supervised fine-tuning). In the final stage of reinforcement learning, the model is optimized for 3,000 steps with a batch size of 1 and a group size  $G = 8$  per GPU. The learning rate is  $5 \times 10^{-6}$  and  $\beta = 0.04$ .

**Evaluation Metrics.** All methods are evaluated on Dreambench [1]. Subject consistency is measured by the cosine

Method	DINO $\uparrow$	CLIP-I $\uparrow$	CLIP-T $\uparrow$
DreamBooth [1]	0.668	0.803	0.305
IP-Adapter [2]	0.696	0.807	0.278
ELITE [29]	0.647	0.772	0.296
BootPIG [30]	0.674	0.797	0.311
OmniGen [31]	0.693	0.801	<b>0.315</b>
OminiControl [3]	0.684	0.799	0.312
Flux.1 IP-Adapter [32]	0.582	0.820	0.288
UNO* [4]	0.717	0.819	0.302
UNO [4]	0.747	0.829	0.303
DreamVAR (Ours)	<b>0.764</b>	<b>0.838</b>	0.310

**Table 1.** Quantitative results on Dreambench. \* indicates models trained on the same data as our DreamVAR.

similarity between the generated and reference subjects in DINO and CLIP feature spaces, denoted as **DINO** and **CLIP-I** scores. Image-text alignment is measured by the cosine similarity between the text prompt and the generated image in CLIP feature space, denoted as the **CLIP-T**.

## 3.2. Experimental Results

**Quantitative Comparisons.** We compare our DreamVAR against existing state-of-the-art methods in Table 1. As shown, despite having only 2B parameters, DreamVAR achieves comparable image-text alignment and superior subject consistency compared to the strong baselines with 12B parameters (i.e., OminiControl and UNO). Notably, our DreamVAR yields the highest DINO (0.764) and CLIP-I (0.838) scores, surpassing all baselines. These results highlight the effectiveness of DreamVAR, reinforced by GRPO, in subject-driven image synthesis, demonstrating its controllability in preserving visual details of reference subjects.

**Qualitative Comparisons.** As shown in Fig. 2, DreamVAR consistently outperforms the other methods. In the first and third rows, IP-Adapter, OmniGen, and OminiControl fail to preserve the appearance of the dog and sneaker, whereas UNO deviates from the prompts. In contrast, DreamVAR produces results that are more faithful to both the appearance and the prompt. In the second row, DreamVAR successfully reconstructs the stuffed animal and aligns with the text, while the other methods fail to preserve its fine-grained details.

## 3.3. Ablation Study and Discussions

**Effect of different rewards.** We conduct an ablation study to evaluate the effect of different reward functions. The results are listed in Table 2. It can be observed that using only subject consistency reward  $R^I$  substantially enhances detail preservation but also reduces image-text alignment. This behavior indicates reward hacking: the model trickly inflates subject consistency reward by directly replicating the reference subject. By additionally incorporating semantic alignment reward  $R^S$ , our full DreamVAR improves the DINO/CLIP-T score from 0.744/0.307 to 0.764/0.310. Fig. 3 further compares the generated images of DreamVAR w/o  $R^S$  and full DreamVAR.



**Fig. 2.** Qualitative comparisons with different methods on Dreambench.



**Fig. 3.** Ablation study of reinforcement learning rewards.

$R^I$	$R^S$	DINO $\uparrow$	CLIP-I $\uparrow$	CLIP-T $\uparrow$
-	-	0.744	0.830	0.307
✓	-	0.810	0.870	0.270
✓	✓	0.764	0.838	0.310

**Table 2.** Ablation study of reinforcement learning rewards.

**Effect of trade-off coefficients in Eq. 4.** We ablate the trade-off coefficients in Eq. 4 by varying their values from 1 to 3. Based on the results in Table 3, we set the default values to  $\alpha = 1.0$  and  $\gamma = 2.0$  to achieve the optimal balance between subject consistency and semantic alignment.

**Effect of multi-scale subject features.** We compare DreamVAR with multi-scale subject features versus last-scale features in Table 4. As shown, using solely last-scale features yields lower DINO and CLIP-I scores compared to the run using multi-scale features, indicating that multi-scale features capture richer details and holistic visual context for better appearance preservation of the reference subject.

**Effect of subject feature pre-filling.** We also compare multi-scale feature injection using the interleaved and our pre-filling strategies in Table 4. It shows that the “Interleaved” strategy lags behind both the “Pre-filling” method and its single-scale variant “Last Scale”. This validates that pre-filling strategy alleviates the train-test discrepancy and improves performance.

**Computational efficiency.** DreamVAR comprises about 2B parameter, which is more compact than UNO (12B). DreamVAR achieves a 1.75 $\times$  training speedup over UNO and reduces inference time from 17 seconds to 2 seconds per image.

$\alpha$	$\gamma$	DINO $\uparrow$	CLIP-I $\uparrow$	CLIP-T $\uparrow$
1.0	1.0	0.770	0.841	0.304
1.0	2.0	0.764	0.838	0.310
1.0	3.0	0.760	0.834	0.308
2.0	1.0	0.774	0.843	0.300
3.0	1.0	0.777	0.846	0.300

**Table 3.** Ablation study of trade-off coefficients in Eq. 4.

	DINO $\uparrow$	CLIP-I $\uparrow$	CLIP-T $\uparrow$
Last Scale	0.734	0.820	0.306
Multiple Scales	0.744	0.830	0.307
Interleaved	0.710	0.812	0.301
Pre-filling	0.744	0.830	0.307

**Table 4.** Ablation study of multi-scale feature pre-filling.

## 4. CONCLUSION

In this work, we investigate the potential of Visual Autoregressive (VAR) models in subject-driven image generation and further validate the efficacy of reinforcement learning in enhancing generation quality within VAR architecture. Specifically, we present DreamVAR, a novel framework that builds upon a text-to-image VAR model. To mitigate the train-test discrepancy inherent in the interleaved conditioning strategy, our DreamVAR pre-fills multi-scale subject features prior to the prediction of target image token sequence. This design simplifies autoregressive dependencies and eliminates the need for joint control-image modeling. We further incorporate Group Relative Policy Optimization to optimize our DreamVAR with subject consistency reward and semantic alignment reward. Extensive experiments demonstrate that our DreamVAR faithfully retains subject details, outperforming state-of-the-art diffusion-based methods.

**Acknowledgements:** This work was supported by the Key Science & Technology Project of Anhui Province (No. 202523009050002) and Basic Research Program of Jiangsu Province (Grant No. BK20243018).

## 5. REFERENCES

- [1] Nataniel Ruiz, Yuanzhen Li, Varun Jampani, Yael Pritch, Michael Rubinstein, and Kfir Aberman, “Dreambooth: Fine tuning text-to-image diffusion models for subject-driven generation,” in *CVPR*, 2023.
- [2] Hu Ye, Jun Zhang, Sibo Liu, Xiao Han, and Wei Yang, “Ip-adapter: Text compatible image prompt adapter for text-to-image diffusion models,” *arXiv preprint arXiv:2308.06721*.
- [3] Zhenxiong Tan, Songhua Liu, Xingyi Yang, Qiaochu Xue, and Xinchao Wang, “Ominicontrol: Minimal and universal control for diffusion transformer,” in *ICCV*, 2025.
- [4] Shaojin Wu, Mengqi Huang, Wenxu Wu, Yufeng Cheng, Fei Ding, and Qian He, “Less-to-more generalization: Unlocking more controllability by in-context generation,” in *ICCV*, 2025.
- [5] Siqi Wan, Jingwen Chen, Qi Cai, Yingwei Pan, Ting Yao, and Tao Mei, “Vton-vllm: Aligning virtual try-on models with human preferences,” in *NeurIPS*, 2025.
- [6] Junyao Gao, Yanan Sun, Yanchen Liu, Yinhao Tang, Yanhong Zeng, Ding Qi, Kai Chen, and Cairong Zhao, “Styleshot: A snapshot on any style,” *IEEE TPAMI*, 2025.
- [7] Jingwen Chen, Yingwei Pan, Ting Yao, and Tao Mei, “Controlstyle: Text-driven stylized image generation using diffusion priors,” in *ACM MM*, 2023.
- [8] Jian Han, Jinlai Liu, Yi Jiang, Bin Yan, Yuqi Zhang, Zehuan Yuan, Bingyue Peng, and Xiaobing Liu, “Infinity: Scaling bit-wise autoregressive modeling for high-resolution image synthesis,” in *CVPR*, 2025.
- [9] Keyu Tian, Yi Jiang, Zehuan Yuan, Bingyue Peng, and Liwei Wang, “Visual autoregressive modeling: Scalable image generation via next-scale prediction,” *NeurIPS*, 2024.
- [10] Qingyang Mao, Qi Cai, Yehao Li, Yingwei Pan, Mingyue Cheng, Ting Yao, Qi Liu, and Tao Mei, “Visual autoregressive modeling for instruction-guided image editing,” *arXiv preprint arXiv:2508.15772*, 2025.
- [11] Aditya Ramesh, Mikhail Pavlov, Gabriel Goh, Scott Gray, Chelsea Voss, Alec Radford, Mark Chen, and Ilya Sutskever, “Zero-shot text-to-image generation,” in *ICML*, 2021.
- [12] Ting Yao, Yehao Li, Yingwei Pan, Zhaofan Qiu, and Tao Mei, “Denoising token prediction in masked autoregressive models,” in *ICCV*, 2025.
- [13] Guangting Zheng, Yehao Li, Yingwei Pan, Jiajun Deng, Ting Yao, Yanyong Zhang, and Tao Mei, “Hierarchical masked autoregressive models with low-resolution token pivots,” in *ICML*, 2025.
- [14] Jonathan Ho, Ajay Jain, and Pieter Abbeel, “Denoising diffusion probabilistic models,” in *NeurIPS*, 2020.
- [15] Robin Rombach, Andreas Blattmann, Dominik Lorenz, Patrick Esser, and Björn Ommer, “High-resolution image synthesis with latent diffusion models,” in *CVPR*, 2022.
- [16] Qi Cai, Jingwen Chen, Yang Chen, Yehao Li, Fuchen Long, Yingwei Pan, Zhaofan Qiu, Yiheng Zhang, Fengbin Gao, Peihan Xu, et al., “Hidream-i1: A high-efficient image generative foundation model with sparse diffusion transformer,” *arXiv preprint arXiv:2505.22705*, 2025.
- [17] Xiang Li, Kai Qiu, Hao Chen, Jason Kuen, Zhe Lin, Rita Singh, and Bhiksha Raj, “Controlvar: Exploring controllable visual autoregressive modeling,” *arXiv preprint arXiv:2406.09750*.
- [18] Jiwoo Chung, Sangeek Hyun, Hyunjun Kim, Eunseo Koh, MinKyu Lee, and Jae-Pil Heo, “Fine-tuning visual autoregressive models for subject-driven generation,” *arXiv preprint arXiv:2504.02612*.
- [19] Zhihong Shao, Peiyi Wang, Qihao Zhu, Runxin Xu, Junxiao Song, Xiao Bi, et al., “Deepseekmath: Pushing the limits of mathematical reasoning in open language models,” *arXiv preprint arXiv:2402.03300*.
- [20] OpenAI, “Gpt-4 technical report,” 2024.
- [21] Mathilde Caron, Hugo Touvron, Ishan Misra, Hervé Jégou, Julien Mairal, Piotr Bojanowski, and Armand Joulin, “Emerging properties in self-supervised vision transformers,” in *ICCV*, 2021.
- [22] Xin Jiang, Ziye Fang, Fei Shen, Junyao Gao, and Zechao Li, “Progressive feature encoding with background perturbation learning for ultra-fine-grained visual categorization,” *IEEE TIP*, 2026.
- [23] An Yang, Bowen Yu, Chengyuan Li, Dayiheng Liu, Fei Huang, Haoyan Huang, Jiandong Jiang, et al., “Qwen2.5-1m technical report,” *arXiv preprint arXiv:2501.15383*.
- [24] Shuai Shao, Zeming Li, Tianyuan Zhang, Chao Peng, Gang Yu, Xiangyu Zhang, Jing Li, and Jian Sun, “Objects365: A large-scale, high-quality dataset for object detection,” in *ICCV*, 2019.
- [25] Black Forest Labs, “Flux,” <https://github.com/black-forest-labs/flux>, 2024.
- [26] Shuai Bai, Keqin Chen, Xuejing Liu, Jialin Wang, Wenbin Ge, Sibo Song, et al., “Qwen2.5-vl technical report,” *arXiv preprint arXiv:2502.13923*.
- [27] Shilong Liu, Zhaoyang Zeng, Tianhe Ren, Feng Li, Hao Zhang, Jie Yang, et al., “Grounding dino: Marrying dino with grounded pre-training for open-set object detection,” in *ECCV*, 2024, pp. 38–55.
- [28] Alexander Kirillov, Eric Mintun, Nikhila Ravi, Hanzi Mao, Chloe Rolland, Laura Gustafson, Tete Xiao, Spencer Whitehead, Alexander C Berg, Wan-Yen Lo, et al., “Segment anything,” in *ICCV*, 2023.
- [29] Yuxiang Wei, Yabo Zhang, Zhilong Ji, Jinfeng Bai, Lei Zhang, and Wangmeng Zuo, “Elite: Encoding visual concepts into textual embeddings for customized text-to-image generation,” in *ICCV*, 2023.
- [30] Senthil Purushwalkam, Akash Gokul, Shafiq Joty, and Nikhil Naik, “Bootpig: Bootstrapping zero-shot personalized image generation capabilities in pretrained diffusion models,” in *ECCV*, 2024.
- [31] Shitao Xiao, Yueze Wang, Junjie Zhou, Huaying Yuan, Xingrun Xing, Ruiran Yan, Chaofan Li, Shuteng Wang, Tiejun Huang, and Zheng Liu, “Omnigen: Unified image generation,” in *CVPR*, 2025.
- [32] InstantX Team, “Instantx flux.1-dev ip-adapter page,” 2024.